Article

Changes in Heavy Oil Saturates and Aromatics in the Presence of Microwave Radiation and Iron-Based Nanoparticles

Alexey V. Vakhin [1,*], Mohammed A. Khelkhal [1,*], Irek I. Mukhamatdinov [1], Rezeda E. Mukhamatdinova [1], Arash Tajik [1], Olga V. Slavkina [2], Sergey Y. Malaniy [2], Marat R. Gafurov [1], Aydar R. Nasybullin [3] and Oleg G. Morozov [3]

[1] Institute of Geology and Petroleum Technologies, Kazan Federal University, 18 Kremlyovskaya Str., 420008 Kazan, Russia; iimuhamatdinov@gmail.com (I.I.M.); rezedat89@mail.ru (R.E.M.); atajik1989@gmail.com (A.T.); mgafurov@gmail.com (M.R.G.)
[2] OJSC RITEK, 85 Lesogorskya St., 400048 Volgograd, Russia; olga.slavkina@lukoil.com (O.V.S.); sergey.malaniy@lukoil.com (S.Y.M.)
[3] Institute of Radio Electronics and Telecommunications, Kazan National Research Technical University Named after A.N. Tupolev-KAI, 10 K. Marx St., 420111 Kazan, Russia; aydar.nasybullin@mail.ru (A.R.N.); microoil@mail.ru (O.G.M.)
*   Correspondence: vahin-a_v@mail.ru (A.V.V.); amine.khelkhal@gmail.com (M.A.K.)

Abstract: Our knowledge of electromagnetic heating's effect on heavy oil upgrading is largely based on very limited data. The aim of the present research was thus to study in detail the effect of microwave exposure in the absence and presence of nanosized magnetite on the composition of heavy oil. The obtained data reveal that the use of nanosized magnetite improves not only microwave radiation application as a result of its absorption and release of thermal energy but also that these nanoparticles have a catalytic ability to break carbon–heteroatom bonds in the composition of resins and asphaltene molecules. In fact, the overall reduction in asphaltenes or resins does not always adequately describe very important changes in asphaltene composition. Even a small fraction of broken carbon–heteroatom bonds can lead to an increase in the mobility of asphaltenes. Moreover, this study has shed light on the important evidence for asphaltenes' transformation, which was found to be the formation of light aromatic compounds, such as alkylbenzenes, naphthalenes and phenanthrenes. These compounds were fixed in the composition of the aromatic fraction. We believe that these compounds could be the fragments obtained from asphaltenes' degradation. The evidence from this study points toward the idea that asphaltenes' destruction is crucial for increasing oil mobility in the reservoir rock during its thermal stimulation.

Keywords: electromagnetic heating; microwave radiations; catalysis; EORs; iron oxide; nanoparticles; aromatics; saturates; heavy oil

1. Introduction

Until now, fossil fuels have been considered as the main source of energy and the basis of world economics. A considerable part of the scientific community considers unconventional oil resources as an alternative to light oil, which has recently witnessed huge consumption and declining reserves [1–3]. A growing body of literature has examined the potential reserves of unconventional oil, which is nowadays classified as heavy and extra-heavy oil. These types of oils are mainly found in Russia, Venezuela and Canada and are characterized by high viscosity, low mobility and high density [4–6]. These features complicate the processes of their extraction and increase the price of their exploitation and processing in addition to increasing environmental pollution.

In general terms, heavy oils are extracted by means of enhanced oil recovery methods (EORs) [7]. These methods are promising in terms of demand satisfaction and environmental protection, especially when they are combined, resulting in less CO_2 emissions

because of the possible use of carbon dioxide as an agent for lowering the surface tension between oil and water in addition to increasing the reservoir pore width [8], or by generating hydrogen from heavy oil components' destruction by the thermal effect or microwave heating [9]. In the literature, there seems to be no general classification of EORs. However, there are three main, widely accepted classes of EORs: chemically, physically and thermally EORs [10–15]. Chemically enhanced oil recovery methods are based on injecting chemicals to increase the mobility of oil within the reservoir. Thermally enhanced oil recovery methods are used to generate heat within the reservoir by burning a part of the oil, such as in the case of in situ combustion [16], or by injecting a water steam, such as in the case of cyclic steam stimulation [17]. On the other hand, physically enhanced oil recovery methods are based on applying electrical methods such as electromagnetic heating via microwave radiation [11].

Among the aforementioned methods, electromagnetic heating is generating considerable interest in terms of decreasing viscosity and increasing oil mobility within low permeability and thermal conductivity reservoirs [18,19]. The first investigation into electromagnetic heating application for enhancing oil recovery reported its possible application not only for heavy and extra-heavy oil reservoirs but for shale oil reservoirs as well [20–22]. What we know about electromagnetic heating is that oscillating at higher frequencies is considerably related to heteroatoms–carbon bond cleavage within heavy oil composition. Moreover, the presence of minerals in the medium has been found to increase the efficiency of microwave radiation intensity and oil generation, which has initiated significant research in the field of applying microwave radiation together with catalytic systems.

It is worth noting that one of the major reasons encouraging the use of the electromagnetic-heating-enhanced oil recovery approach is the damage of reservoirs resulting from the use of other enhanced oil recovery techniques such as thermal or chemical enhanced oil recovery. Furthermore, using classical enhanced oil recovery (chemical or thermal) for a long period of time generates a serious accumulation of paraffins near the well, which, as a consequence, may affect the production operation and hydrocarbon transportation as well. Moreover, the use of microwave radiation could, on the one hand, replace the use of steam injection methods, which consume more energy and time [23], and on the other hand, could be suitable for reservoirs with low permeability. However, one of the main drawbacks to adopting microwave radiation for the exploitation of heavy oil reservoirs is the need to maintain the reservoir temperature to promote recovery continuity in addition to corrosion, which may result from reservoirs with high salinity [24,25].

An alternative solution, though less exhaustive, is the application of microwave radiation along with catalytic systems [18,26]. This method represents a viable alternative to classical enhanced oil recovery, where the distributed catalysts within the reservoir could stimulate the entire area by microwave radiation and maintain its temperature at a fixed value. Various catalysts have been proposed to enhance heavy oil recovery with different properties and characteristics. These catalysts have been classified into water-soluble, oil-soluble and dispersed nanoparticles [27–33]. Broadly speaking, different enhanced oil recovery methods have demonstrated a significant positive effect of nanoparticles on heavy oil upgrading [34–37]. The iron-based nanoparticles are recognized as being the most promising catalysts in terms of improving heavy oil compounds' conversion under the thermal effect and in terms of being able to control them from the surface due to their electromagnetic properties [38].

The present paper gives a brief overview of the effect generated by the application of iron-based nanoparticles coupled with the use of microwave radiation on heavy oil saturates' and aromatic compounds' composition. The first section examines the research object and the applied investigation methods. The second section discusses the data obtained from the application of the obtained catalyst to improve the efficiency of the microwave radiation process and ends with the obtained conclusions.

2. Results and Discussions

Catalyst's Precursor Activation

The obtained catalyst was characterized by Mössbauer, XRD and SEM analysis, as shown in Figure 1. The obtained data show nanoparticles of Fe_3O_4 less than 200 nm in size as witnessed in the SEM image and confirmed by Mössbauer and XRD data.
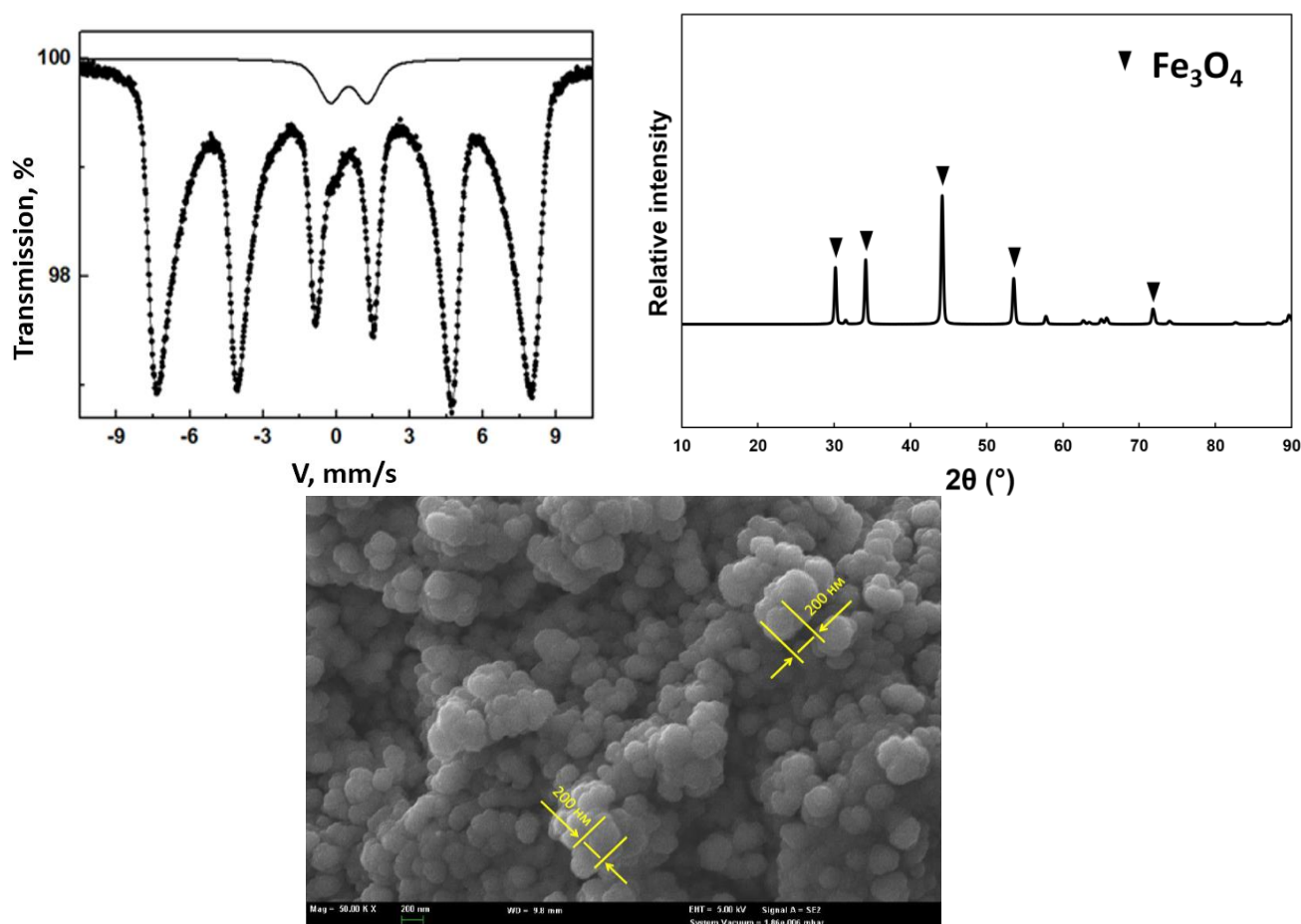

Figure 1. Mössbauer, XRD and SEM analysis of the obtained catalyst.

So that we would be able to study the effect of microwave heating in the presence of iron oxide nanoparticles, we used the A. N. Tupolev laboratory stand at Kazan National Research Technical University to study the effect of the microwave-absorbing particles presented in the schematic diagram of Figure 2. As can be seen, in one of the maxima of the E field, there was a test tube which contained the oil sample, with nanosized magnetite particles distributed throughout. The frequency of electromagnetic oscillations was 2.45 GHz, and the output power of the generator in continuous mode was 700–800 W.

The iron oxide particles were distributed in 1/10 of the oil sample volume using an ultrasonic homogenizer in order to eliminate the effect on the oil bulk area. Next, this oil sample was mixed with another oil without a catalyst in a ratio of 1/10. As a result, we obtained a 1 to 100 catalyst–oil ratio. The control experiments were carried out without catalyst particles under similar conditions. Generally, the experiments were carried out at a power of 1 kW for 3 min. On the other hand, resinous–asphaltene substances were found to have to have the greatest ability to absorb microwave radiation in the absence of water in the composition of oil samples. SARA analysis of the initial oil, processed oil with microwave radiation and the catalytic process in the presence of microwave radiation are provided in Table 1.
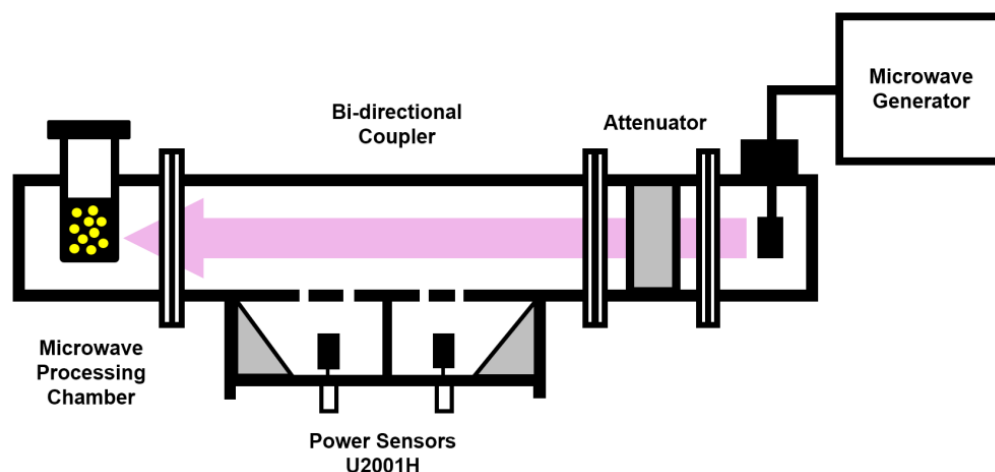
Figure 2. Schematic diagram of the laboratory stand applied for studying the effect of microwave heating with iron oxide nanoparticles on heavy oil composition changes.

Table 1. SARA and elemental analysis of oil samples in the absence and presence of iron oxide nanoparticles under microwave radiation.

Sample			Abbreviation	SARA Fractions, wt.%				Elemental Compositions, wt.%				
				Saturates	Aromatics	Resins	Asphaltenes	C	H	N	S	O
Initial heavy oil				23.9	39.2	29.2	7.9	82.1	10.1	0.6	2.6	4.6
MW-Processed heavy oil	Non-catalytic MW-processed heavy oil		MW(E)	25.7	36.4	30.7	7.2	82.4	9.9	0.6	2.4	4.7
	Catalytic MW-processed heavy oil	Place for Electric field	MW(E) + Fe_3O_4	30.7	43.8	19.4	6.1	82.8	10.2	0.6	2.0	4.4
		Place for Magnetic field	MW(H) + Fe_3O_4	30.3	37.2	25.5	7.0	82.3	10.1	0.6	2.1	4.9

According to elemental analysis, sulfur content changed significantly. It is well-known that the weakest C-S bonds in the composition of resins and asphaltenes are primarily subjected to destruction under the thermal effect. The non-catalytic MW-processed heavy oil did not show significant changes in SARA analysis. However, in the presence of the catalyst, the content of asphaltenes was reduced by 20%. Moreover, changes in the resin content were found to be more significant. In addition, relatively to the non-catalytic MW-processed heavy oil, the resin content was reduced from 30.7 wt.% to 19.4 wt.%. Interestingly, the processing in the magnetic field also led to changes in heavy oil SARA analysis, but to a lesser extent. Furthermore, the content of asphaltenes slightly changed relatively to the resin content, which decreased from 30.7 wt.% to 25.5 wt.% as indicated in Table 1. It is common knowledge that the content of resins and asphaltenes is very important even if their content varies slightly. In fact, the destruction of asphaltenes often occurs through carbon–sulfur bonds in bridge structures [39]. This can provide a significant reduction in the molecular weight of asphaltenes, and the resulting fragments increase the content of saturated and aromatic hydrocarbon fractions. Therefore, the viscosity of oil decreased after microwave exposure (Figure 3).

To be able to study this phenomenon, we applied GCMS to study the composition of these fractions. The chromatograms of the saturated fraction (Figure 4) show changes in the samples after microwave exposure in the presence of iron oxide nanoparticles; changes in the relative content of both normal alkanes and isoalkanes were observed. On the chromatograms, the height of the peaks changes abruptly; isoalkanes predominate. It can also be seen that after microwave exposure, there was an increase in the number of n-alkanes with a longer chain of composition of $C_{21}H_{44}$-$C_{29}H_{60}$, wherein the maximum falls on hexacosan $C_{26}H_{54}$.
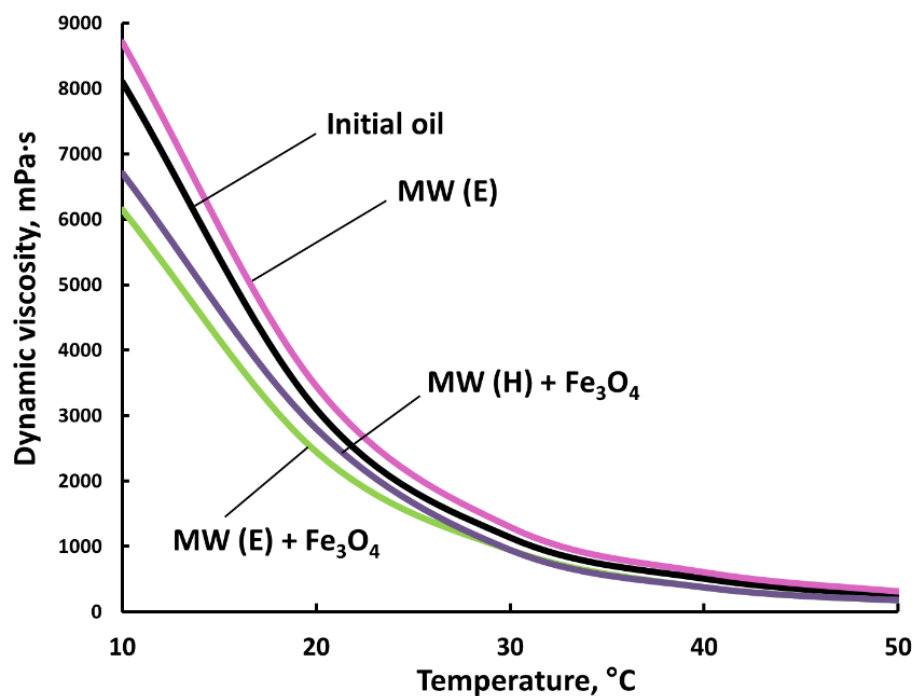
Figure 3. Oil viscosity dependence on temperature before and after MW processing.
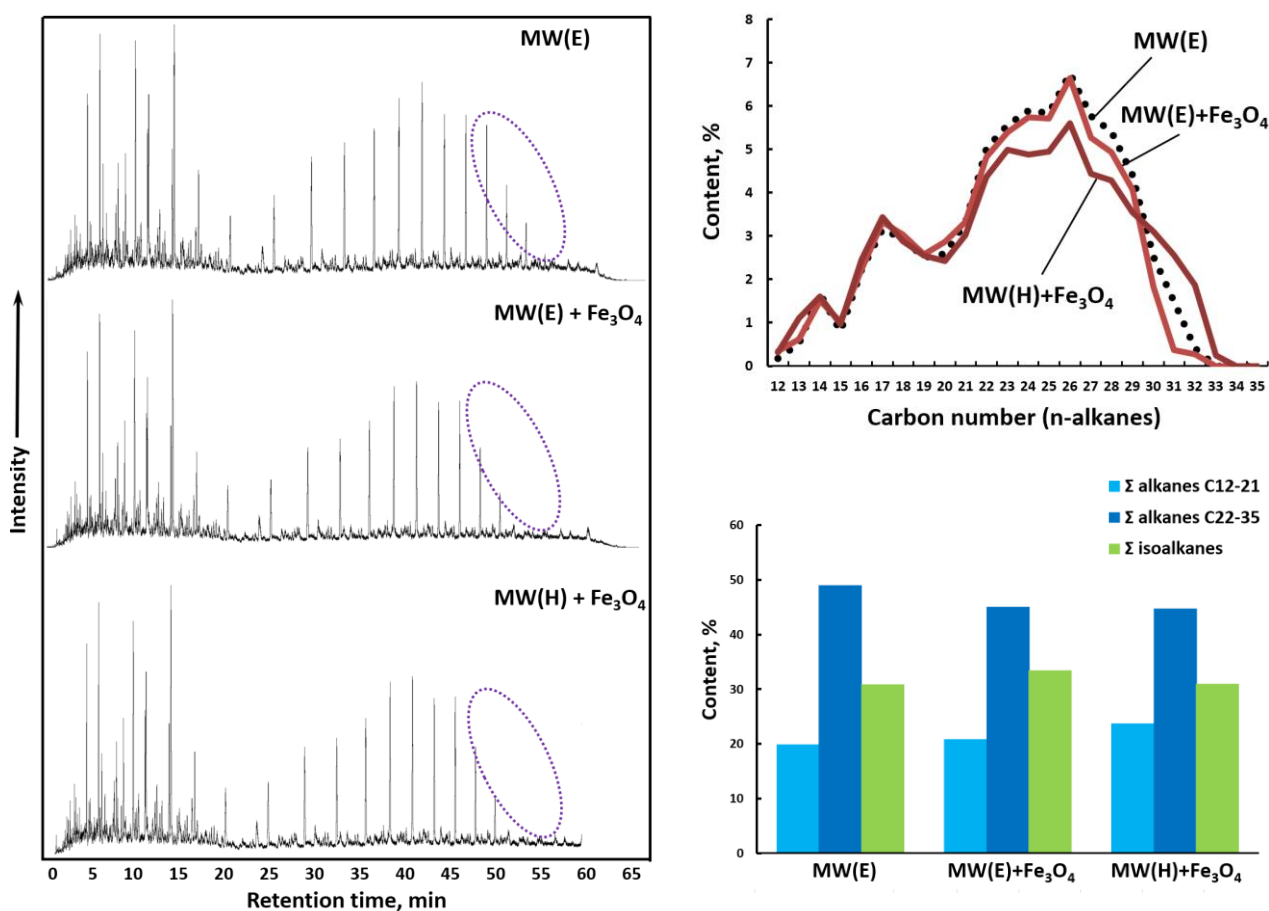
Figure 4. Chromatograms of saturated hydrocarbons C_{10}-C_{32}—the number of carbon atoms in n-alkanes, iC_{13}-iC_{18}—i-alkanes. The relative content of normal alkanes in the studied oil samples after exposure to a microwave field. In the lower-right corner—a change in the content of the sum of n-alkanes and isoalkanes.

The chromatogram of the sample after exposure to a microwave field at the maximum electric field in the presence of magnetite particles differs from the chromatogram of the sample without the catalyst—in other words, the relative content of phytane ($C_{20}H_{42}$) increased, and the content of alkanes with a chain length of C_{22}-C_{32} slightly decreased.

The chromatogram of the sample exposed to the maximum magnetic field with magnetite differs slightly from that of the control experiment exposed to the maximum electric field. In this case, there was a slight increase in the relative content of alkanes with a chain length of C_{12}-C_{20} and a decrease in C_{22}-C_{29} alkanes. However, the content of C_{30}-C_{32} alkanes increased. It can be assumed that as a result of microwave exposure, radical addition reactions occurred in the control sample, resulting in the formation of alkanes with a longer hydrocarbon chain. Nevertheless, with the combination of microwave exposure and the catalytic effect of magnetite, there was a slight decrease in alkanes with a composition of C_{21} and higher, while the relative content of C_{12}-C_{20} alkanes increased.

Figure 4 also shows diagrams of changes in the relative content of alkanes in the studied oil samples. An increase in the number of n-alkanes occurred as a result of the destruction of resin and asphaltene molecules due to the abstraction of aliphatic substituents, as well as dealkylation reactions of cyclic saturated and aromatic hydrocarbons [40–42]. Figure 4 shows how the relative content of the sum of alkanes and isoalkanes changed. Compared to the control exposure to the electric component of the microwave field, in samples with the addition of magnetite, there was a slight increase in the relative content of isoalkanes and alkanes with the composition C_{12}-C_{21}, while the content of alkanes with a longer chain decreased.

Table 2 presents data on the geochemical coefficients of the studied samples. The most significant changes were observed for the C_{27}/C_{17} ratio. The proportion of alkanes with an average molecular weight increased. This was the result of the generation of medium-molecular-weight alkanes during the destruction of aliphatic substituents in asphaltenes. In addition, the cracking reactions of C-C bonds with the formation of lighter products had already begun at temperatures equal to 250 °C and higher [43].

Table 2. Geochemical coefficients of the studied oil samples after experiments.

Geochemical Coefficients	Without Catalyst. Place for Electric Field Processing	With Catalyst	
		Place for Electric Field Processing	Place for Magnetic Field Processing
	MW(E)	MW(E) + Fe_3O_4	MW(H) + Fe_3O_4
Pristane/Phytane	0.52	0.52	0.68
Pr/C_{17}	1.57	1.55	1.72
Ph/C_{18}	3.22	3.28	3.02
C_{27}/C_{17}	**1.82**	**1.58**	**1.29**
$\Sigma(C_{27}-C_{31})/\Sigma(C_{15}-C_{19})$	1.69	1.35	1.46
$\Sigma(C_{12}-C_{21})/\Sigma(C_{22}-C_{30})$	0.41	0.54	0.52
$2nC_{29}/(C_{28} + C_{30})$	1.11	1.21	0.96

The chromatograms of the aromatic fraction of the studied samples were studied in detail with the ions recording *m/z* 50-500 (TIC), ions *m/z* 133 for alkylbenzenes, *m/z* 128, 142 and 156 for naphthalene and its homologues and *m/z* 178, 192 and 206 for phenanthrene and its homologues. To assess possible changes, computer reconstruction of chromatograms was carried out using fragment ions characteristic of various groups of hydrocarbons to determine the effect of the microwave field on individual groups of compounds, such as alkylbenzenes, naphthalenes and phenanthrenes. It was found that these compounds could be the fragments of the degraded asphaltenes. Moreover, the destruction of asphaltenes is very important for increasing the mobility of heavy oil in the dense porous medium of the reservoir rock. The overall reduction in asphaltenes or tars does not always adequately describe very important changes in the composition of asphaltenes. Even a small fraction of broken carbon–heteroatom bonds can lead to an increase in the mobility of asphaltenes.

Such processes are evidenced by the formation of light aromatic hydrocarbons, which are fixed in the composition of the aromatic fraction. Chromatograms of the alkylbenzenes (Figure 5) of all studied samples are almost identical. The graph shows the relative content of 1,3,4-trimethyl-2-alkylbenzenes.
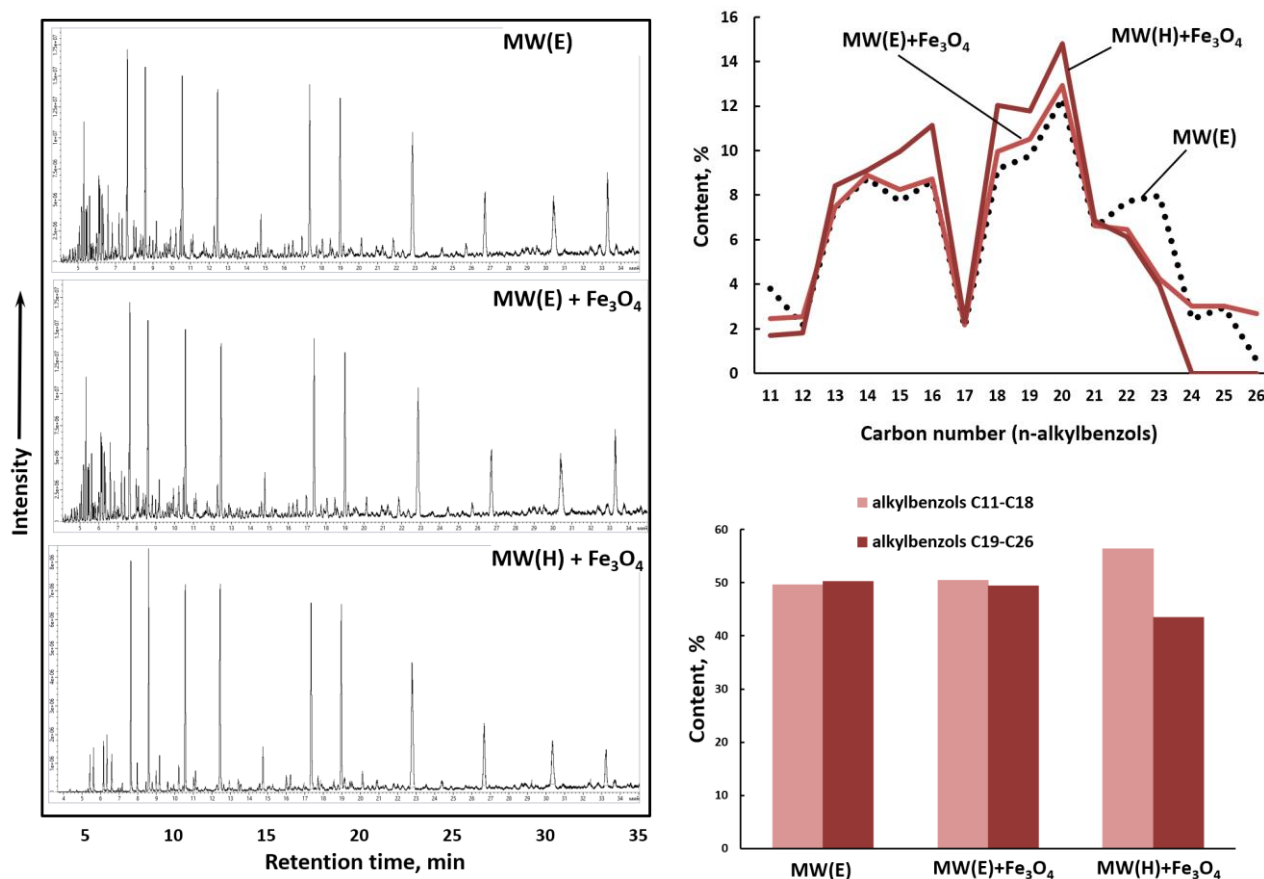

Figure 5. Chromatograms and relative contents of 1,3,4-trimethyl-2-alkylbenzenes in the aromatic fraction of oil samples after microwave exposure. In the lower-right corner is the ratio between long-chain and short-chain alkylbenzenes.

The chromatograms of naphthalene and its methyl-substituted homologues (Figure 6) show slight changes. Compared to the control sample, on the chromatogram of the sample after exposure to the microwave in the presence of magnetite, the relative content of naphthalene itself and its methyl-, dimethyl- and ethyl-substituted homologues is higher, and the relative content of trimethylnaphthalenes is lower. On the chromatogram of the sample after microwave exposure with the catalyst, the changes are more significant compared to the control sample: the relative content of naphthalene and methylnaphthalenes is very low, the content of trimethylnaphthalenes is higher. The graph also (Figure 6) shows the relative contents of naphthalene and its homologues in the studied samples. In the presence of the catalyst and upon exposure to the electrical component of the field, the content of naphthalene and its homologues was significantly higher than in other samples. An increase in the content of naphthalene homologues is a sign that, as a result of microwave exposure, the destruction of heavy compounds with a more complex structure, such as resins and asphaltenes, occurs. Furthermore, a higher content of dimethylnaphthalenes compared to tri- and monomethylnaphthalenes occurs during the demethylation reactions of tri- and tetrasubstituted naphthalenes [42].
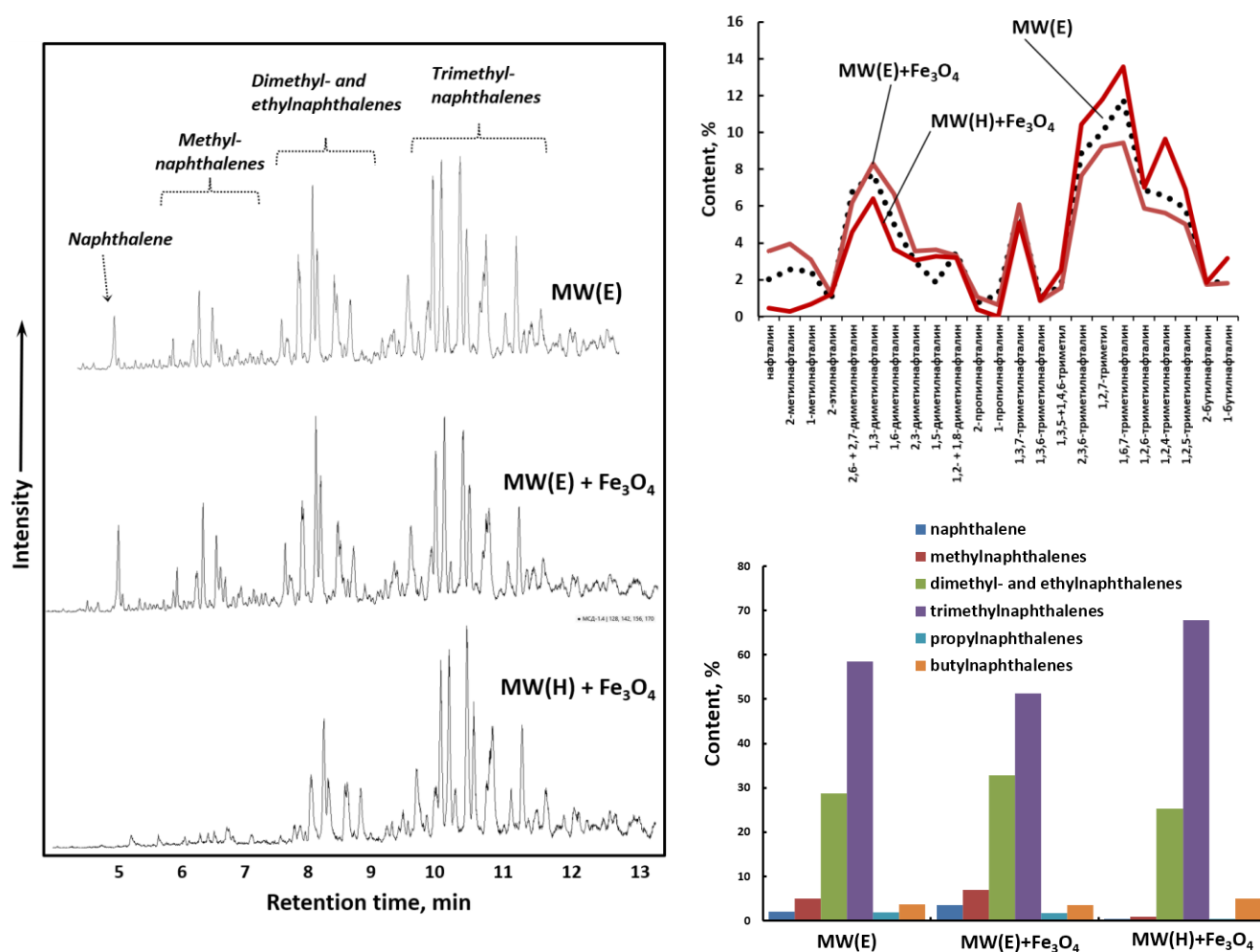
Figure 6. Chromatograms and relative contents of naphthalene and its homologues in the aromatic fraction of the studied oil samples after exposure to microwave radiations. In the lower-right corner—changes in the content of naphthalene and its homologues.

The chromatograms of phenanthrene and its methyl-substituted homologues of the studied samples are almost identical. There were only slight changes in the content of dimethylnaphthalenes, which are clearly visible in Figure 7. An increase in the content of phenanthrene and its homologues was the result of demethylation reactions, which means that such processes did not occur in this case. The processes of transformation of the composition of heavy oil under the influence of a microwave field in the absence and presence of the catalyst that combines the functions of a microwave field absorber have been studied. Changes in the composition of oil caused by the process of destructive hydrogenation of resinous–asphaltene substances intensified in the presence of nanosized magnetite particles were established. The degradation products of resinous–asphaltene substances are fixed in the fractions of saturated and aromatic hydrocarbons. Injection of nanosized magnetite can be carried out in the oil-bearing rock in the form of iron tallates, followed by their decomposition and the formation of nanosized iron oxide particles. Iron oxide particles have a high chemical affinity for mineral compounds and are retained on the rock during oil filtration.
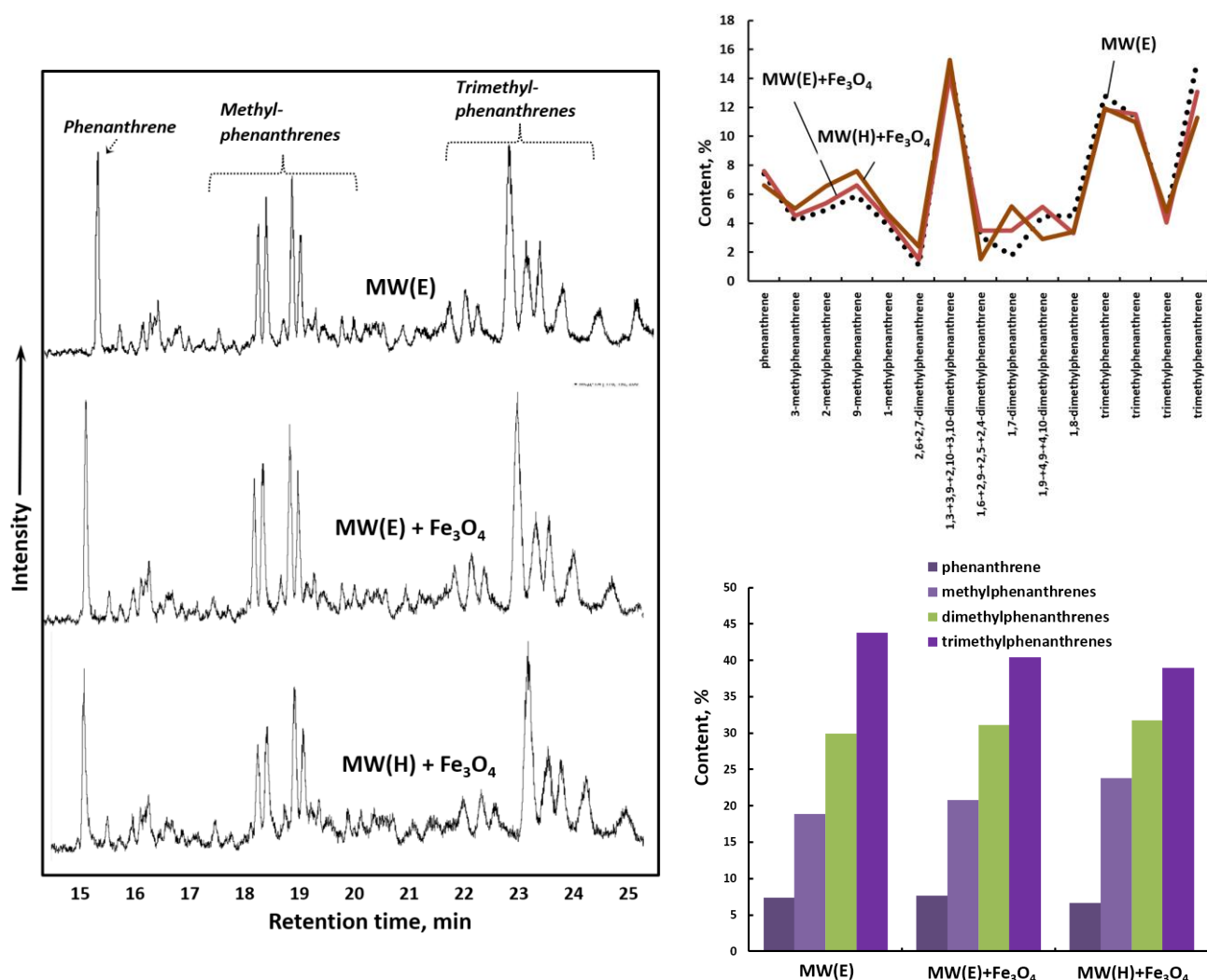
Figure 7. Chromatograms and relative contents of phenanthrene and its homologues in the aromatic fraction of the studied oil samples after exposure to microwave exposure. In the lower-right corner—changes in the content of phenanthrene and its homologues.

3. Experimental Section

3.1. Object of Research

In the present study, we used a heavy oil sample obtained from the Ashal'cha field in the Republic of Tatarstan (Russia).

3.2. Catalytic Agent

In order to study the effect of iron-based nanoparticles, we used nanodispersed magnetite particles 100–200 nm in size. After the experiments, the catalyst particles were separated from the oil by centrifugation at 5000 rpm. The dispersion and morphology of the obtained magnetite are characterized by a set of physical methods.

3.2.1. X-ray Diffraction Analysis

The X-ray diffraction analysis was accomplished using Shimadzu XRD-7000S automatic powder diffractometer (Kyoto, Japan) using a nickel monochromator with a step of 0.008 nm and 3 s of exposure, in combination with a Bruker D2 PHaser and CuKα radiation with a wavelength of $\lambda = 1.54060$ nm.

3.2.2. Scanning Electron Microscope (SEM) Analysis

SEM analysis was carried out on a field-emission scanning electron microscope Merlin from Carl Zeiss (Oberkochen, Germany) equipped with an energy-dispersive X-ray spectrometer (EDX mapping) Aztec X-Max from Oxford Instruments to study the morphology and elemental composition of catalyst particles. Before proceeding to microscope observation, the studied samples were transferred to carbon scotch and loaded in a vacuum chamber. The surface morphology was analyzed on secondary electron mode, with a very high resolution (0.8nm). Elemental analysis was performed under 20 keV with the angle selective backscatter mode to reveal the difference in composition.

3.2.3. Mössbauer Spectroscopy

The Mössbauer spectra were obtained using the MS-1104 Em spectrometer in the continuous acceleration mode at room temperature using a symmetric sawtooth law of velocity change with separate accumulation of the spectra as the source moves forward and backward and subsequent summation to eliminate background line distortion. A scintillation counter with a thin NaJ(Tl) crystal was used as a detector. The spectra were obtained with a ^{57}Co source in the Rh matrix. Calibration was performed using the α-Fe spectrum, and isomer shifts were measured from the "center of gravity" of the spectrum obtained at room temperature of this reference. Mathematical handling of the gained spectra was carried out through the standard Mössbauer program UnivemMS, 2021.

3.3. Dynamic Viscosity Measurements

The determination of viscosity–temperature characteristics of the initial oil from the Ashal'cha oil field and the oils after experiments was carried out using a FUNGILAB Alpha L rotational viscometer (Valencia, Spain) equipped with an adapter with a thermostatically controlled jacket. The required temperature in the thermal jacket was maintained using a HUBER MPC K6 cooling thermostat. The determination of viscosity–temperature characteristics was carried out at temperatures ranging from 10 to 50 °C with a step of 10 °C by using 6.7 mL of sample volume in a TL5 spindle. The shear rate for this spindle was determined by the formula 1.32*RPM (according to the device passport). The RPM was determined for a specific temperature and spring torque from 50 to 90%. The relative error of the FUNGILAB viscometer did not exceed ±1.0%, and the reproducibility was 0.2%.

3.4. SARA Analysis

Based on ASTM D2007 recommendations, we separated the initial oil and the samples obtained after microwave radiation in the presence of the catalyst into saturates, aromatics, resins and asphaltenes. The aforementioned method includes asphaltene precipitation with an oil–hexane ratio of 1:40. We chose hexane to maintain light fractions in maltenes. Furthermore, maltenes were separated into four fractions: saturates were eluted with hexane via liquid adsorption chromatography using aluminum oxide previously calcined at 420 °C. Aromatics and resins were obtained by toluene and a mixture of benzene and isopropyl alcohol (1:1), respectively.

3.5. Gas Chromatography–Mass Spectroscopy (GC-MS)

The saturate and aromatic fractions obtained from the experiments were analyzed by a GC-MS system, which included the gas GC "Chromatech-Crystal 5000" (Moscow, Russia) with a mass-selective detector ISQ (USA). The obtained results were processed by the Xcalibur application. Firstly, a capillary column 30 m in length with a diameter of 0.25 mm was used for performing the experiments. The carrier gas was helium with a flow rate of 1 mL/min at a temperature of 310 °C. The adjusted thermostat regime started with a rise from 100 °C to 150 °C with a heating rate of 3 °C/min, from 150 °C to 300 °C with a heating rate of 12 °C/min, followed by its isotherm, which continued until the end of the analysis. Finally, the electron energy was 70 eV, and the ion source temperature was set to

250 °C. Saturate and aromatic fractions' elements were identified by means of NIST Mass Spectral Library and literature sources.

3.6. Elemental Analysis

The elemental composition of the studied heavy oil samples was measured by X-ray fluorescence method, in M4 Tornado from Bruker. These types of analysis provided data on the content of C, H, N, O and S in the samples of heavy oil.

4. Conclusions

In summary, we carried out experiments on changes in heavy oil saturates and aromatics in the presence of microwave radiation and iron-based nanoparticles. The evidence from this study suggests that heavy oil SARA fractions and their chemical composition significantly change under the effect of microwave radiation in the presence of iron oxide nanoparticles. This effect was studied in detail in the present study. The obtained data have not only revealed that the use of nanosized magnetite improves microwave radiation application as a result of its absorption and release of thermal energy but also that these nanoparticles have a catalytic ability to break carbon–heteroatom bonds in the composition of resins and asphaltene molecules. The present study has revealed that the overall reduction in asphaltenes or resins does not always adequately describe crucial changes in asphaltene composition. It has also been found that the mobility of asphaltenes is highly dependent on carbon–heteroatom bonds breaking, where even a small fraction may lead to a significant increase in it. In addition, this study provided further evidence for the transformation of asphaltenes into light aromatic compounds, such as alkylbenzenes, naphthalenes and phenanthrenes, which were fixed in the composition of the aromatic fraction. Our findings would seem to demonstrate that these compounds are fragments of asphaltenes' degradation, which supports the idea that asphaltenes' destruction plays a major role in increasing oil mobility in the reservoir rock under thermal processing. This study has led us to conclude that the injection of iron oxide nanoparticles into heavy oil formations can be carried out in the form of oil-soluble iron compounds such iron tallates with subsequent decomposition into nanosized iron oxide particles. The established patterns of the influence of a catalytic reagent on the composition of heavy oil justify a fundamentally new approach to modernizing the electrical-based enhanced oil recovery methods for heavy oil reservoirs. These observations could lead to an increase in heavy oil recovery and an improvement of its chemical composition.

References

1. Toma, S.H.; Santos, J.J.; da Silva, D.G.; Huila, M.F.G.; Toma, H.E.; Araki, K. Improving stability of iron oxide nanofluids for enhanced oil recovery: Exploiting wettability modifications in carbonaceous rocks. *J. Pet. Sci. Eng.* **2022**, *212*, 110311. [CrossRef]
2. Board, N.E. *Canada's Oil Sands Opportunities and Challenges To 2015: An Update*; National Energy Board: Calgary, AB, Canada, 2006; ISBN 066243353X.
3. Jia, C. Breakthrough and significance of unconventional oil and gas to classical petroleum geological theory. *Shiyou Kantan Yu Kaifa/Petroleum Explor. Dev.* **2017**, *44*, 1–11. [CrossRef]
4. Zheng, R.; Liu, D.; Tang, J.; Song, Q.; Yao, Q. Analysis of montmorillonite affecting coke formation during the thermal conversion of heavy oil. *Fuel* **2021**, *288*, 119687. [CrossRef]
5. Alvarado, V.; Manrique, E. Enhanced oil recovery: An update review. *Energies* **2010**, *3*, 1529–1575. [CrossRef]
6. Panait-Patica, A.; Serban, D.; Ilie, N.; Pavel, L.; Barsan, N. Suplacu de Barcau Field-A Case History of a Successful In-Situ Combustion Exploitation. In Proceedings of the SPE Europec/EAGE Annual Conference and Exhibition, Society of Petroleum Engineers, Vienna, Austria, 12–15 June 2006; p. 10.
7. Gholami, Z.; Gholami, F.; Tišler, Z.; Vakili, M. A Review on the Production of Light Olefins Using Steam Cracking of Hydrocarbons. *Energies* **2021**, *14*, 8190. [CrossRef]
8. Aycaguer, A.-C.; Lev-On, M.; Winer, A.M. Reducing carbon dioxide emissions with enhanced oil recovery projects: A life cycle assessment approach. *Energy Fuels* **2001**, *15*, 303–308. [CrossRef]
9. Mehlman, S. *Carbon Capture and Sequestration (via Enhanced Oil Recovery) from a Hydrogen Production Facility in an Oil Refinery*; Praxair, Incorporated: Danbury, CT, USA, 2010.
10. Tirado, A.; Yuan, C.; Varfolomeev, M.A.; Ancheyta, J. Kinetic modeling of aquathermolysis for upgrading of heavy oils. *Fuel* **2022**, *310*, 122286. [CrossRef]
11. Rehman, M.M.; Meribout, M. Conventional versus electrical enhanced oil recovery: A review. *J. Pet. Explor. Prod. Technol.* **2012**, *2*, 169–179. [CrossRef]
12. Thomas, S. Enhanced oil recovery-an overview. *Oil Gas Sci. Technol. l'IFP* **2008**, *63*, 9–19. [CrossRef]
13. Sheng, J.J. *Modern Chemical Enhanced Oil Recovery*; Gulf Professional Publishing: Burlington, VT, USA, 2011; ISBN 9781856177450.
14. Brandt, A.R.; Unnasch, S. Energy intensity and greenhouse gas emissions from thermal enhanced oil recovery. *Energy Fuels* **2010**, *24*, 4581–4589. [CrossRef]
15. Al-Muntaser, A.A.; Varfolomeev, M.A.; Suwaid, M.A.; Feoktistov, D.A.; Yuan, C.; Klimovitskii, A.E.; Gareev, B.I.; Djimasbe, R.; Nurgaliev, D.K.; Kudryashov, S.I.; et al. Hydrogen donating capacity of water in catalytic and non-catalytic aquathermolysis of extra-heavy oil: Deuterium tracing study. *Fuel* **2021**, *283*, 118957. [CrossRef]
16. Khelkhal, M.A.; Eskin, A.A.; Sharifullin, A.V.; Vakhin, A.V. Differential scanning calorimetric study of heavy oil catalytic oxidation in the presence of manganese tallates. *Pet. Sci. Technol.* **2019**, *37*, 1194–1200. [CrossRef]
17. Mukhamatdinov, I.I.; Salih, I.S.S.; Khelkhal, M.A.; Vakhin, A.V. Application of Aromatic and Industrial Solvents for Enhancing Heavy Oil Recovery from the Ashalcha Field. *Energy Fuels* **2020**, *35*, 374–385. [CrossRef]
18. Vakhin, A.V.; Khelkhal, M.A.; Tajik, A.; Gafurov, M.R.; Morozov, O.G.; Nasybullin, A.R.; Karandashov, S.A.; Ponomarev, A.A.; Krapivnitskaia, T.O.; Glyavin, M.Y. The Role of Nanodispersed Catalysts in Microwave Application during the Development of Unconventional Hydrocarbon Reserves: A Review of Potential Applications. *Processes* **2021**, *9*, 420. [CrossRef]
19. Hascakir, B.; Babadagli, T.; Akin, S. Experimental and Numerical Modeling of Heavy-Oil Recovery by Electrical Heating. In Proceedings of the International Thermal Operations and Heavy Oil Symposium, Society of Petroleum Engineers, Calgary, AB, Canada, 20–23 October 2008.
20. Baptist, O.C. *Oil Recovery and Formation Damage in Permafrost, Umiat Field, Alaska*; U.S. Department of the Interior, Bureau of Mines: Washington, DC, USA, 1960; Volume 5642.
21. Zhou, Z.; Gunter, W.D.; Kadatz, B.; Cameron, S. Effect of clay swelling on reservoir quality. *J. Can. Pet. Technol.* **1996**, *35*, 07. [CrossRef]
22. Bailey, S.A.; Kenney, T.M.; Schneider, D.R. Microbial Enhanced Oil Recovery: Diverse Successful Applications of Biotechnology in the Oil Field. In Proceedings of the SPE Asia Pacific Improved Oil Recovery Conference, Society of Petroleum Engineers, Kuala Lumpur, Malaysia, 8–9 October 2001.
23. Taheri-Shakib, J.; Shekarifard, A.; Naderi, H. Experimental investigation of comparing electromagnetic and conventional heating effects on the unconventional oil (heavy oil) properties: Based on heating time and upgrading. *Fuel* **2018**, *228*, 243–253. [CrossRef]
24. Vakhin, A.V.; Khelkhal, M.A.; Tajik, A.; Ignashev, N.E.; Krapivnitskaya, T.O.; Peskov, N.Y.; Glyavin, M.Y.; Bulanova, S.A.; Slavkina, O.V.; Schekoldin, K.A. Microwave Radiation Impact on Heavy Oil Upgrading from Carbonate Deposits in the Presence of Nano-Sized Magnetite. *Processes* **2021**, *9*, 2021. [CrossRef]
25. Sierra, R.; Tripathy, B.; Bridges, J.E.; Ali, S.M. Promising progress in field application of reservoir electrical heating methods. In Proceedings of the SPE International Thermal Operations and Heavy Oil Symposium, Society of Petroleum Engineers, Porlamar, Venezuela, 12–14 March 2001.
26. Li, H.; Gao, H.; Zhao, X.; Xia, Z.; Yu, B.; Sun, D. Experimental study on viscosity reduction of heavy oil with water content by synergistic effect of microwave and nano-catalyst. *J. Pet. Sci. Eng.* **2022**, *208*, 109271. [CrossRef]
27. Boukherissa, M.; Mutelet, F.; Modarressi, A.; Dicko, A.; Dafri, D.; Rogalski, M. Ionic liquids as dispersants of petroleum asphaltenes. *Energy Fuels* **2009**, *23*, 2557–2564. [CrossRef]

28. Li, Y.-B.; Gao, H.; Pu, W.-F.; Li, L.; Chen, Y.; Bai, B. Study of the catalytic effect of copper oxide on the low-temperature oxidation of Tahe ultra-heavy oil. *J. Therm. Anal. Calorim.* **2019**, *135*, 3353–3362. [CrossRef]

29. Kniazeva, M.; Maximov, A. Effect of Additives on the Activity of Nickel–Tungsten Sulfide Hydroconversion Catalysts Prepared In Situ from Oil-Soluble Precursors. *Catalysts* **2018**, *8*, 644. [CrossRef]

30. Kok, M.V. The thermal characterization of crude oils in a limestone matrix of different particle size. *Energy Sources Part A Recover. Util. Environ. Eff.* **2014**, *36*, 923–928. [CrossRef]

31. Guo, K.; Li, H.; Yu, Z. In-situ heavy and extra-heavy oil recovery: A review. *Fuel* **2016**, *185*, 886–902. [CrossRef]

32. Mukhamatdinov, I.I.; Salih, I.S.; Vakhin, A.V. Changes in the subfractional composition of heavy oil asphaltenes under aquathermolysis with oil-soluble CO-based catalyst. *Pet. Sci. Technol.* **2019**, *37*, 1589–1595. [CrossRef]

33. Salih, I.S.S.; Mukhamatdinov, I.I.; Vahin, A.V.; Garifullina, E.I. Fractional composition of heavy oil asphaltenes of volga-ural petroleum province. *Int. Multidiscip. Sci. GeoConf. SGEM Surv. Geol. Min. Ecol. Manag.* **2017**, *17*, 485–491.

34. Khelkhal, M.A.; Eskin, A.A.; Nurgaliev, D.K.; Vakhin, A.V. Thermal study on stabilizing combustion front via bimetallic Mn@Cu tallates during heavy oil oxidation. *Energy Fuels* **2019**, *34*, 5121–5127. [CrossRef]

35. Farhadian, A.; Khelkhal, M.A.; Tajik, A.; Lapuk, S.E.; Rezaeisadat, M.; Eskin, A.A.; Rodionov, N.O.; Vakhin, A.V. Effect of Ligand Structure on the Kinetics of Heavy Oil Oxidation: Toward Biobased Oil-Soluble Catalytic Systems for Enhanced Oil Recovery. *Ind. Eng. Chem. Res.* **2021**, *60*, 14713–14727. [CrossRef]

36. Khelkhal, M.A.; Lapuk, S.E.; Ignashev, N.E.; Eskin, A.A.; Glyavin, M.Y.; Peskov, N.Y.; Krapivnitskaia, T.O.; Vakhin, A.V. A Thermal Study on Peat Oxidation Behavior in the Presence of an Iron-Based Catalyst. *Catalysts* **2021**, *11*, 1344. [CrossRef]

37. Sitnov, S.; Mukhamatdinov, I.; Aliev, F.; Khelkhal, M.A.; Slavkina, O.; Bugaev, K. Heavy oil aquathermolysis in the presence of rock-forming minerals and iron oxide (II, III) nanoparticles. *Pet. Sci. Technol.* **2020**, *38*, 574–579. [CrossRef]

38. Qi, H.; Jiang, H.; You, Y.; Hu, J.; Wang, Y.; Wu, Z.; Qi, H. Mechanism of Magnetic Nanoparticle Enhanced Microwave Pyrolysis for Oily Sludge. *Energies* **2022**, *15*, 1254. [CrossRef]

39. Korneev, D.S.; Pevneva, G.S.; Golovko, A.K. Thermal transformations of asphaltenes in heavy oils at 120 °C. *J. Sib. Fed. Univ. Chem.* **2019**, *12*, 101–117.

40. Golovko, A.K.; Grin'ko, A.A. Structural Transformations of Petroleum Resins and Their Fractions by Thermolysis. *Pet. Chem.* **2018**, *58*, 599–606. [CrossRef]

41. Korneev, D.S.; Pevneva, G.S.; Voronetskaya, N.G. Effects of the Composition and Molecular Structure of Heavy Oil Asphaltenes on Their Reactivity in Thermal Decomposition Processes. *Pet. Chem.* **2021**, *61*, 152–161. [CrossRef]

42. Voronetskaya, N.G.; Pevneva, G.S.; Korneev, D.S.; Golovko, A.K. Influence of asphaltenes on the direction of thermal transformations of heavy oil hydrocarbons. *Pet. Chem.* **2020**, *60*, 166–173. [CrossRef]

43. Montgomery, W.; Court, R.W.; Rees, A.C.; Sephton, M.A. High temperature reactions of water with heavy oil and bitumen: Insights into aquathermolysis chemistry during steam-assisted recovery. *Fuel* **2013**, *113*, 426–434. [CrossRef]